

ITEM RESPONSE SCALING LAWS: A MEASUREMENT THEORY APPROACH TO GENERALIZABLE NEURAL PERFORMANCE PREDICTION

Anonymous authors

Paper under double-blind review

ABSTRACT

Classical neural scaling laws describe how the performance of large language models (LLMs) improves with increased compute, but they are typically estimated in aggregate across all questions in a benchmark, overlooking the information carried by individual questions. Item Response Theory (IRT) offers a principled way to address this by modeling per-question characteristics, though traditional IRT is limited to binary data with a Bernoulli loss. In pre-training downstream scaling, probabilities of producing the correct answer over the entire vocabulary yield more informative laws, while in test-time scaling, repeated sampling naturally gives rise to empirical probabilities. Empirical probability responses do not arise in human testing or LLM leaderboard evaluations, settings where IRT has shown success. To bridge this gap, we propose extending IRT with a Beta loss on empirical probability responses, naturally yielding Item Response Scaling Laws. We validate our framework in two large-scale studies: (1) pre-training downstream scaling, using 25 models from 6 families with up to 359 checkpoints on 15 NLP datasets; and (2) test-time scaling, using 15 models on 10 NLP datasets with up to 10,000 samples per question. In both cases, IRT-based approaches provide reliable and efficient estimates of scaling behavior while remaining interpretable and generalizable.¹

1 INTRODUCTION

Modern large language models (LLMs) are general-purpose tools that offer diverse capabilities. Scaling laws, such as pre-training downstream scaling and test-time scaling, provide a principled framework for understanding and improving LLM performance. Pre-training downstream scaling laws characterize how a model’s performance on downstream tasks improves as a function of the computational effort invested during pre-training, typically measured in floating-point operations (FLOP) (Biderman et al., 2023; Mishra et al., 2024). Test-time scaling laws describe how a model’s inference performance on a benchmark (e.g., success rate) grows with the number of stochastic samples performed at test time (Brown et al., 2024; Hughes et al., 2024).

Deriving these scaling laws requires extensive data; however, practical studies are constrained to small experimental scales due to their costly nature. As a baseline, LLM evaluation leaderboards typically involve on the order of 10^6 questions evaluated across 10^2 models, amounting to 10^8 total queries (Liang, 2023). Based on this, pretraining downstream scaling laws introduce around 10^2 pretraining checkpoints per model, and test-time scaling laws introduce around 10^4 samples per question. These additional dimensions inflate the total number of queries by several orders of magnitude. Consequently, existing studies often evaluate only a limited set of models and a subset of benchmark questions, and they rely primarily on mean score as the performance metric (Chen et al., 2024; Schaeffer et al., 2024; Brown et al., 2024).

The laws derived from limited experimental scales can exhibit surprising and unintuitive behaviors, including inconsistencies across different model–benchmark pairs. For example, Brown et al. (2024) derives a power-law test-time scaling relationship that, as Schaeffer et al. (2025) demonstrates, holds only for ill-structured response distributions in single-sample success rates. Such phenomena suggest that the benchmark-specific factors, such as the difficulty of each question, play a crucial role in shaping the scaling behavior. Moreover, mean score on a subset may not reliably reflect overall

¹Code: anonymous.4open.science/r/irsl-7560

	Definition	Classical Fitting Approach	IRT-based Fitting Approach
Pre-training Acc	$\mathbb{E}[\text{Acc}(i, \mathcal{D})] = \frac{1}{N} \sum_{j=1}^N p_{ij}$	$a \cdot \sigma(b \cdot (\alpha \cdot \text{FLOP}_i^{-\beta} + \gamma - c)) + d$	$\frac{1}{N} \sum_{j=1}^N \sigma(f(\text{FLOP}_i) - z_j)$
Pre-training $p_{\text{Correct Choice}}$	$p_{\text{Correct Choice}}(i, \mathcal{D}) = \frac{1}{N} \sum_{j=1}^N p_{\text{Correct Choice}}(i, j)$	$g(\text{FLOP}_i)$	$\frac{1}{N} \sum_{j=1}^N \sigma(f(\text{FLOP}_i) - z_j)$
Test-time	$\text{pass}@k(i, \mathcal{D}) = \frac{1}{N} \sum_{j=1}^N 1 - (1 - p_{ij})^k$	$\exp(-a \cdot k^{-b})$	$\frac{1}{N} \sum_{j=1}^N (1 - (1 - \sigma(\theta_i - z_j))^k)$

Table 1: The definitions, classical fitting approach, and IRT-based fitting approach for Acc, $p_{\text{Correct Choice}}$ (downstream pre-training scaling law), and pass@k (test-time scaling law). We use the Rasch model as a demonstration. Classical fitting approaches fit uninterpretable parameters specific to datasets and LLMs. Our IRT-based fitting approach learns question-level parameters (rather than dataset-level ones), while being interpretable and generalizable.

performance, nor does mean score on one dataset generalize to other datasets with similar measurement objectives but different difficulty levels (Truong et al., 2025). More fundamentally, these shortcomings arise because prevailing scaling-law formulations implicitly treat datasets as homogeneous inputs and focus exclusively on aggregate metrics, thereby obscuring the heterogeneity of item characteristics.

Item Response Theory (IRT), originating from psychology and educational testing, offers a principled way to address these limitations. IRT parameterizes question-level characteristics to model the probability that a test taker (human or LLM) answers a question correctly. It is typically applied in two phases: calibration and computerized adaptive testing (CAT). In the calibration phase, a binary response matrix is collected from test takers (human or LLMs) and used to estimate item characteristics such as question difficulty. With these calibrated parameters, CAT adaptively selects informative subsets of questions to reliably and efficiently evaluate new test takers. IRT has been highly successful in human testing, and recent work has shown its promise on binary response data from LLM leaderboards (Biderman et al., 2023; Mishra et al., 2024; Magnusson et al., 2025; Gadre et al., 2024). However, in both pre-training downstream scaling and test-time scaling laws, there is a need to model empirical probabilities rather than binary responses, an aspect absent from both human testing and LLM leaderboard evaluations. In the pre-training setting, mean scores often exhibit emergent behaviors and poor predictability (Lourie et al., 2025), whereas probabilities of producing the correct answer over the entire vocabulary preserve richer information and yield more consistent scaling laws (Schaeffer et al., 2024). In the test-time setting, repeated sampling naturally gives rise to empirical probabilities. Motivated by this, we propose extending IRT with a Beta loss to model empirical probabilities, yielding efficiently estimated, interpretable, and generalizable Item Response Scaling Laws. Our contributions are:

- We conduct a large-scale study on 25 models from 6 model families, ranging from 111M to 13B parameters, with up to 359 pretraining checkpoints, on 15 popular natural language datasets, to demonstrate the superiority of our item response pretraining downstream scaling laws: interpretable, generalizable, and giving robust estimates of the scaling behavior with limited budgets.
- We conduct a large-scale study on 15 models across 10 popular natural language datasets with up to 10,000 repeated sampling steps. We demonstrate that IRT gives more reliable estimates of the scaling behavior in an efficient manner, surpassing traditional approaches, while being interpretable and generalizable.

By embedding the scaling law within the IRT framework, our approach provides a theoretically principled and empirically validated alternative to conventional aggregate performance scaling.

2 RELATED WORK

Pre-training Downstream Scaling Law Many neural networks exhibit power-law scaling of the pre-training loss as a function of the amount of compute, data, or parameters used for training (Hestness et al., 2017; Kaplan et al., 2020; Bahri et al., 2021; Hernandez et al., 2021; Hoffmann et al., 2022; Muennighoff et al., 2024). Unlike predicting loss, predicting downstream performance from scale is generally harder (Lourie et al., 2025; Schaeffer et al., 2024). However, recent work has demonstrated it can be done based on a two-step prediction that chains together predictions from

scale to loss and loss to downstream performance (Biderman et al., 2023; Mishra et al., 2024; Magnusson et al., 2025; Gadre et al., 2024).

Test-time Scaling Law Test-time scaling laws characterize how a model’s performance on a benchmark (e.g., success rate) improves as the number of stochastic samples drawn at inference increases (Brown et al., 2024; Hughes et al., 2024). Schaeffer et al. (2025) demonstrate that such laws hold only for ill-structured response distributions in single-sample success rates. Kang et al. (2025) develop scalable test-time inference strategies that balance sample efficiency and performance gains under limited budgets. Dorner et al. (2025) establish that the shape of a verifier’s ROC curve governs the effectiveness of rerolling and best-of-N, formalizing limits of test-time scaling with imperfect verifiers. Zhang et al. (2025) survey the test-time scaling literature and outline open challenges for reliability and generalization.

Measurement Theory-based AI evaluation Several recent works adopt Item Response Theory (IRT) as a foundation for AI evaluation using binary responses and Bernoulli loss (Truong et al., 2025; Hofmann et al., 2025; Kipnis et al., 2025; Madaan et al., 2024; Polo et al., 2024). Polo et al. (2025) introduce Sloth scaling laws, which model benchmark performance through low-dimensional latent skills influenced by compute, offering a measurement-theoretic perspective that improves prediction and interpretability across LLM families. Heineman et al. (2025) propose a framework based on signal and noise to quantify benchmark reliability, showing that higher signal-to-noise ratios correlate with more accurate model ranking and lower scaling law prediction error, and introducing interventions to improve evaluation robustness.

3 METHOD

Item Response Theory (IRT) provides an elegant and parsimonious mathematical framework to model the natural interaction of LLMs and benchmark questions. We show how, under this framework, various known scaling laws arise naturally and how the framework facilitates efficient, interpretable, and generalizable scaling evaluation. We show the definitions, classical fitting approaches, and IRT-based fitting approaches of the scaling laws in Table 1.

3.1 ITEM RESPONSE THEORY

Item Response Theory refers to a class of probabilistic latent variable models that explain the relationship between the test taker’s latent ability, the question’s characteristics (e.g., difficulty), and the observed response from the test taker to the questions (Baker, 2001; Van der Linden et al., 2000). A central model in IRT is the Rasch model (Rasch, 1993), where each test-taker (here, an LLM) has an ability parameter θ , and each question has a difficulty parameter z . A higher θ denotes greater ability, while a higher z signifies a more difficult question. Let y denote the response of the test taker to the question, where $y = 1$ if the response is correct and 0 otherwise. The probability of a correct response is modeled by $p(y = 1 | \theta, z) = \sigma(\theta - z)$, where σ is the sigmoid function. Another widely adopted model in IRT is the 2PL model (Lord, 1952; Birnbaum, 1968), which adds a discrimination parameter a to capture how sharply a question differentiates between test-takers of different abilities, modeling the probability of a correct response as $p(y = 1 | \theta, z, a) = \sigma(a(\theta - z))$. In this case, A higher a indicates that the question is more effective at distinguishing between abilities close to its difficulty level. The difficulty z and the discrimination a are collectively referred to as the item parameters. The use of IRT consists of two phases: calibration, which estimates item parameters, and computerized adaptive testing (CAT), which enables efficient evaluation for new test-takers.

In traditional human testing, the most common approach is to perform calibration on binary response data, where each question is scored as either correct or incorrect. A binary response matrix $Y \in \{0, 1\}^{M \times N}$ is collected, where M and N denote the number of test takers and questions, respectively. Each entry Y_{ij} represents a response of test taker i to question j . With the binary response matrix, the item parameters can be estimated via either MLE or EM by minimizing the Bernoulli loss between the IRT-predicted probabilities and the observed binary responses $\mathcal{L}_{\text{Bernoulli}} = - \sum_{i=1}^M \sum_{j=1}^N [Y_{ij} \log p_{ij} + (1 - Y_{ij}) \log(1 - p_{ij})]$ (Bock & Aitkin, 1981; Chalmers, 2012; Wu et al., 2020).

Unlike human testing, LLM evaluation provides empirical response probabilities, which convey richer information than binary responses. In the pre-training downstream scenario, the probability of producing the correct answer among the entire vocabulary, $p^{\text{Vocab}}(\text{Correct Choice})$, as well as among the set of multiple-choice options, $p^{\text{Choices}}(\text{Correct Choice})$, provides a richer signal than accuracy of

binary responses (Schaeffer et al., 2024). In the test-time scaling scenario, each question is queried thousands of times with independent samples to estimate pass@1 , defined as the probability that a single independent sample answers the question correctly. To exploit those probability information for calibration, we collect the probability matrix $P \in \mathbb{R}^{M \times N}$, $0 \leq P_{ij} \leq 1$ and estimate the item parameters by minimizing the Beta loss between the IRT-predicted probabilities and the observed empirical probabilities $\mathcal{L}_{\text{Beta}} = -\sum_{i=1}^M \sum_{j=1}^N \log(\text{BetaPDF}(P_{ij}; \mu_{ij}, \phi))$, where $\mu_{ij} = p_{ij}$ is the IRT-predicted probability, and ϕ is a precision (inverse variance) parameter. Traditional calibration on binary data usually demands a large and diverse set of LLMs, which is costly to obtain. By leveraging empirical response probabilities, reliable calibration can be achieved with fewer test-takers, thereby significantly lowering the computational cost of querying LLMs.

Given a question bank \mathcal{Q} with calibrated item parameters, computerized adaptive testing can efficiently evaluate new test-takers using fewer questions. At query step t , given the current estimate of the test taker’s ability θ_{new}^t and the calibrated item parameters, the next question q_j^{*t} is selected as the most informative question, guided by an acquisition function such as Fisher information \mathbb{I} (Meijer & Nering, 1999; Chang, 2015; Magis et al., 2017). This process iterates between the question selection step $q_j^{*t} = \arg \max_{q_j \in \mathcal{Q}^t} \mathbb{I} \quad \mathcal{Q}^{t+1} = \mathcal{Q}^t \setminus \{q_j^{*t}\}$ and the ability estimation step $\theta_{\text{new}}^{t+1} = \arg \max_{\theta_{\text{new}}^t} \sum_{j=1}^t \log p_{\text{new},j}$. Ability estimation can also be carried out using binary responses with a Bernoulli loss or empirical probability responses with a Beta loss.

3.2 PRE-TRAINING DOWNSTREAM ITEM RESPONSE SCALING LAW

The pre-training downstream scaling law characterizes how model performance on a benchmark scales with the compute used during model pre-training. Performance of model i on dataset \mathcal{D} (e.g., MMLU) with N questions indexed by j is usually quantified by the expected mean accuracy, which is often approximated with an empirical mean accuracy:

$$\begin{aligned} \mathbb{E}[\text{Acc}(i, \mathcal{D})] &= \mathbb{E}\left[\frac{1}{N} \sum_{j=1}^N Y_{ij}\right] = \frac{1}{N} \sum_{j=1}^N \mathbb{E}[Y_{ij}] = \frac{1}{N} \sum_{j=1}^N p_{ij}. \\ \mathbb{E}[\text{Acc}(i, \mathcal{D})] &\approx \text{Acc}(i, \mathcal{D}) = \frac{1}{N} \sum_{j=1}^N Y_{ij}, \text{ where } Y_{ij} \sim \text{Bern}(p_{ij}). \end{aligned} \tag{1}$$

The binary variable Y_{ij} is model i ’s response to the j -th question (1 for a correct response and 0 otherwise). Classical linear approximation model Acc as a function of the model i ’s pretraining compute FLOP_i (Bhagia et al., 2024; et al., 2024; Gadre et al., 2024).

$$\text{Acc}(i, \mathcal{D}) \approx a \cdot \sigma(b \cdot (L_i - c)) + d \text{ where } L_i \approx \alpha \cdot \text{FLOP}_i^{-\beta} + \gamma, \tag{2}$$

where σ is the sigmoid function, a, b, c , and d are dataset-specific parameters for \mathcal{D} , L_i is the LLM-specific cross-entropy loss, and α, β, γ are LLM-specific parameters for model i . None of these scaling parameters is interpretable.

We propose to model the probability of test taker i correctly answering question j from benchmark \mathcal{D} with IRT. For example, under the Rasch model, this probability is given as $\hat{p}_{ij} = \sigma(\theta_i - z_j)$:

$$\mathbb{E}[\text{Acc}(i, \mathcal{D})] \approx \frac{1}{N} \sum_{j=1}^N \hat{p}_{ij} = \frac{1}{N} \sum_{j=1}^N \sigma(\theta_i - z_j) \quad \theta_i = f(\text{FLOP}_i), \tag{3}$$

where θ_i generalizes across questions that measure the same construct, and z_j generalizes across different LLMs. θ_i can be interpreted as the ability of test taker i , z_j can be interpreted as difficulty of question j . Modeling pre-training downstream scaling law from Acc gives emergent behavior and low predictability (Lourie et al., 2025; Schaeffer et al., 2024). There is growing interest in modeling the law from the probability of producing the correct answer among the entire vocabulary, $p^{\text{Vocab}}(\text{Correct Choice})$, which preserves more information (Schaeffer et al., 2024):

$$p_{\text{Correct Choice}}(i, \mathcal{D}) = \frac{1}{N} \sum_{j=1}^N p_{\text{Correct Choice}}(i, j). \tag{4}$$

Traditional approaches tend to fit a regression model with LLM-specific and dataset-specific parameters g : $p_{\text{Correct Choice}}(i, \mathcal{D}) \approx g(\text{FLOP}_i)$. We propose to use IRT to model $p_{\text{Correct Choice}}(i, j)$. For example, under the Rasch model, this probability is given as $p_{\text{Correct Choice}}(i, j) = \sigma(\theta_i - z_j)$:

$$p_{\text{Correct Choice}}(i, \mathcal{D}) \approx \frac{1}{N} \sum_{j=1}^N \sigma(\theta_i - z_j), \quad \theta_i = f(\text{FLOP}_i). \quad (5)$$

3.3 TEST-TIME ITEM RESPONSE SCALING LAW

Test-time scaling investigates the predictable relationship between a model’s success rates on a benchmark and the number of independent samples generated during inference (Brown et al., 2024; Hughes et al., 2024). The model i ’s success rate on dataset \mathcal{D} with N questions indexed by j and H samples indexed by k is quantified by $\text{pass@k}(i, \mathcal{D})$:

$$\text{pass@k}(i, \mathcal{D}) = \frac{1}{N} \sum_{j=1}^N \text{pass@k}(i, j) = \frac{1}{N} \sum_{j=1}^N 1 - (1 - \text{pass@1}(i, j))^k \quad (6)$$

where the $\text{pass@k}(i, j) = 1$ if at least one of the k generated responses of model i to q_j is correct, and $\text{pass@1}(i, j)$ denote the probability that a single independent sample of model i correctly answers question q_j (Schaeffer et al., 2025). Brown et al. (2024) model the negative log success rate falls as a power law with the number of independent samples k : $\text{pass@k}(i, \mathcal{D}) \approx \exp(-ak^{-b})$, where $a, b > 0$ are uninterpretable model-specific and benchmark-specific parameters. We propose to model $\text{pass@1}(i, j)$ using IRT. For example, under the Rasch model, this probability is given by $\text{pass@1}(i, j) = p_{ij} = \sigma(\theta_i - z_j)$. Instead of fitting LLM-specific and benchmark-specific constants a, b , we model $\text{pass@k}(i, \mathcal{D})$ as a function of IRT parameters:

$$\text{pass@k}(i, \mathcal{D}) \approx \frac{1}{N} \sum_{j=1}^N \left(1 - (1 - \hat{p}_{ij})^k\right) = \frac{1}{N} \sum_{j=1}^N \left(1 - (1 - \sigma(\theta_i - z_j))^k\right), \quad (7)$$

where θ_i generalizes across questions that measure the same construct, and z_j generalizes across different LLMs, both are interpretable.

4 EXPERIMENTS

We demonstrate the advantages of the downstream item response scaling law in Section 4.1 and of the test-time item response scaling law in Section 4.2.

4.1 PRE-TRAINING DOWNSTREAM ITEM RESPONSE SCALING LAW

Experimental Setup We collect two sets of responses across LLMs and datasets. (1) The first consists of the binary responses from 13 models spanning 3 model families with up to 359 checkpoints, evaluated on 13 datasets covering both exact-match and multiple-choice tasks. This yields a binary response matrix Y_1^{pretrain} . The data are queried using the HELM framework at temperature 0 (Liang, 2023). Truong et al. (2025) calibrated question difficulties on these datasets using the Rasch model with binary responses from 42–91 diverse LLMs on the HELM leaderboard. Under the same query setup, we reuse these calibrated difficulties in our experiments. (2) The second is obtained from Schaeffer et al. (2024) and contains outputs from 5 model families (see Schaeffer et al. (2024) for details). For our experiments, we select three out of the 12 multiple-choice datasets in Schaeffer et al. (2024). Each output includes a binary response y , a probability response $p^{\text{Vocab}}(\text{Correct Choice})$, and a probability response $p^{\text{Choices}}(\text{Correct Choice})$, resulting in one binary response matrix Y_2^{pretrain} and two probability response matrices $P_2^{\text{pretrain pvocab}}$ and $P_2^{\text{pretrain pchoices}}$. The data are queried using the LM Evaluation Harness at temperature 0 (Gao et al., 2023). Hofmann et al. (2025) calibrate item parameters on these datasets using the 2PL model with binary responses from 102 diverse LLMs on the Open LLM Leaderboard (Beeching et al., 2023). Under the same query setup, we reuse these calibrated item parameters in our experiments.

Binary-IRT CAT and Scaling Law Fit We first apply IRT with a Bernoulli loss (denoted Binary-IRT) to the binary response matrix Y_1^{pretrain} . Using the calibrated question difficulties, we conduct CAT on the LLM checkpoints with a question budget of 100. We then compare the θ -FLOP curve

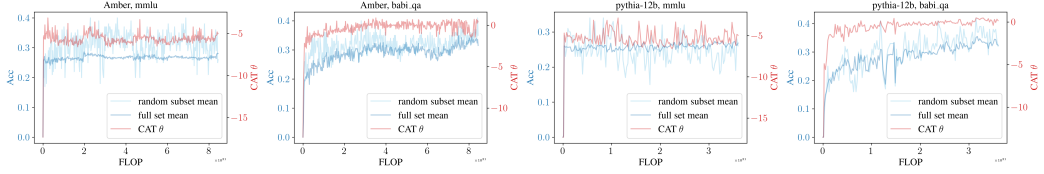


Figure 1: Comparison of binary-IRT (red) and Acc curves (light blue) during pre-training on a subset, across 2 LLMs and 2 datasets. The full-set Acc (dark blue) serves as ground truth. The blue lines use the left y -axis (Acc), while the red line use the right y -axis (CAT θ). Subset binary-IRT yields lower variance than subset Acc. But both IRT and ground truth Acc show emergent behavior and exhibit poor predictability.

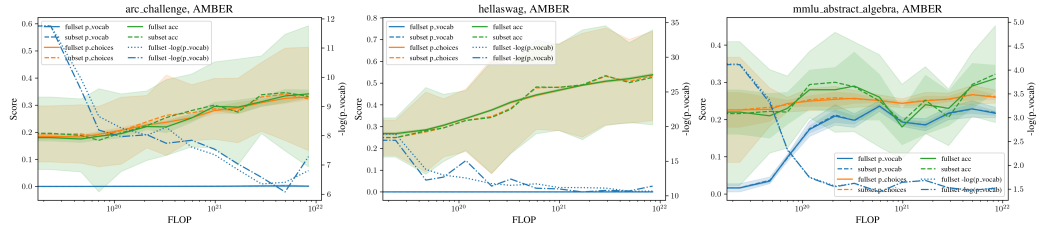


Figure 2: Naive scaling behavior of three metrics (Acc, $p^{\text{Vocab}}(\text{Correct Choice})$, $p^{\text{Choices}}(\text{Correct Choice})$) versus FLOP of AMBER on 3 datasets. Because $p^{\text{Vocab}}(\text{Correct Choice})$ is often too small to visualize, we also plot its negative log probability. The left y -axis corresponds to the three metrics, and the right y -axis corresponds to $-\log p^{\text{Vocab}}$. Shaded regions indicate ± 3 standard deviations estimated from subset sampling or bootstrap. $p^{\text{Vocab}}(\text{Correct Choice})$ or its negative log probability does not show emergent behaviors and exhibits strong predictability.

obtained from CAT with the Acc–FLOP curve computed on a random subset of 100 questions. The full-set Acc serves as the ground truth. As shown in Figure 1, IRT yields lower variance and closely tracks the ground-truth curve. To assess evaluation stability, we report the total variation (TV) following Hofmann et al. (2025). For each model i and benchmark \mathcal{D} with V checkpoints, let $x_i^v(\mathcal{D})$ denote the measured performance (either Acc or θ) at checkpoint v . The normalized total variation is defined as $\text{TV}(i, \mathcal{D}) = \frac{V}{V-1} \cdot \frac{\sum_{v=1}^{V-1} |x_i^{v+1}(\mathcal{D}) - x_i^v(\mathcal{D})|}{|x_i^V(\mathcal{D}) - x_i^1(\mathcal{D})|}$, where lower values indicate lower step-to-step variance and thus higher evaluation quality. Averaged across all datasets and models, subset Acc yields $\text{TV} = 39.66$, while subset IRT achieves $\text{TV} = 26.72$, demonstrating its superior stability. However, neither IRT nor ground truth Acc addresses the challenging questions of downstream scaling laws: emergence and predictability.

Naive Scaling Behavior of $p^{\text{Correct Choice}}$ Schaeffer et al. (2024) find that $p^{\text{Vocab}}(\text{Correct Choice})$ retains substantially more information than binary responses, offering a potential avenue to address emergence and predictability. Using Y_2^{pretrain} , $P_2^{\text{pretrain pvocab}}$, and $P_2^{\text{pretrain pchoices}}$, we examine the naive scaling behavior of three metrics: Acc, $p^{\text{Vocab}}(\text{Correct Choice})$, and $p^{\text{Choices}}(\text{Correct Choice})$. Figure 2 plots these metrics against FLOP of AMBER on three datasets, averaged across the full set and on a random subset of 50 questions. We observe that $p^{\text{Vocab}}(\text{Correct Choice})$ (or its negative log) exhibits clear scaling behavior. While $p^{\text{Vocab}}(\text{Correct Choice})$ is too small to be effectively modeled by IRT on ARC Challenge and HellaSwag, it appears feasible on MMLU. Accordingly, we apply Beta-IRT to both $p^{\text{Vocab}}(\text{Correct Choice})$ and $p^{\text{Choices}}(\text{Correct Choice})$ for MMLU. Moreover, the average $p^{\text{Vocab}}(\text{Correct Choice})$ across the 50-question subset of MMLU closely aligns with the full-set curves with low variance, suggesting that naive probability-based metrics already provide strong approximations that may be difficult for IRT to improve upon, as we describe next.

Beta-IRT CAT and Scaling Law Fit We apply IRT with a Beta loss (denoted Beta-IRT) to the probability response matrix $P_2^{\text{pretrain pvocab}}$ and $P_2^{\text{pretrain pchoices}}$. Using the calibrated item parameters, we conduct CAT on the LLM checkpoints with a question budget of 50. In Figure 3, we use the average $p^{\text{Vocab}}(\text{Correct Choice})$ on the full set as the ground truth. We compare the average $p^{\text{Correct Choice}}$ on the subset, and estimate θ using Beta-IRT CAT on probability responses with the budget. We

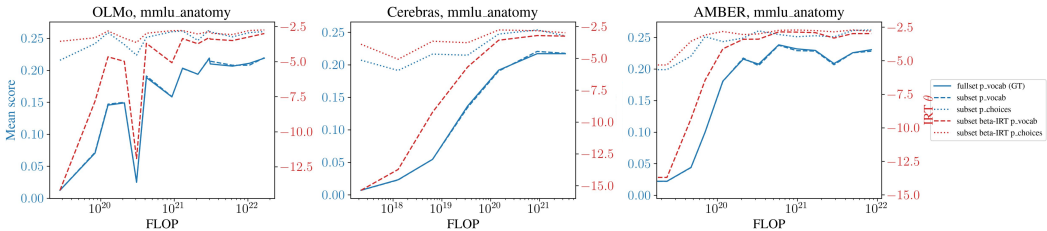


Figure 3: Scaling behavior of three model families on MMLU Anatomy. The blue lines use the left y -axis (Mean score), while the red lines use the right y -axis (IRT θ). Beta-IRT effectively captures $p_{\text{Correct Choice}}$, which is more predictable and less emergent.

observe that both the θ estimated from Beta-IRT CAT and the average $p_{\text{Correct Choice}}$ exhibit smooth increasing trends that closely align with the ground truth. This suggests that Beta-IRT effectively captures $p_{\text{Correct Choice}}$, which is more predictable and less emergent, making it a suitable candidate for modeling downstream scaling laws. We note, however, that while subset Beta-IRT does not surpass the subset average of $p_{\text{Correct Choice}}$ in estimation accuracy or stability, it performs comparably and remains valuable for its interpretability and generalizability, as we describe next.

IRT Ability Estimates Generalize across Questions Measuring the same Construct

We use the scaling performance of Pythia-12B on WikiFact (from Y_1^{pretrain}) as a demonstration. The scaling law is characterized by the relationship between Acc and the training FLOP of the 154 Pythia-12B checkpoints. We split the questions into an easy subset for training and a difficult subset for testing according to the calibrated difficulties. For the IRT model, we first estimate the model’s ability parameter θ on the training set using pre-calibrated difficulties; we then model θ as a function of FLOP via Kernel Ridge Regression: $\theta = f_{\text{KRR}}(\text{FLOP})$. Finally, we infer the test set accuracy by combining $f_{\text{KRR}}(\text{FLOP})$ with the pre-calibrated test set difficulties. As shown in Figure 4, the IRT model closely matches the ground truth curve on both the training and test sets. This shows that θ generalizes across questions with different difficulties but measuring the same construct, while the traditional scaling law remains test set-specific. We replicate this experiment across 13 benchmarks and 13 models from Y_1^{pretrain} . Figure 7 presents the difference in test mean squared error (MSE) with ground truth between the classical scaling law (which fits on the train ground truth and stays the same for the test set) and the item response scaling law (which generalizes to the test set). From the consistent positive MSE difference, we conclude that the item response scaling law demonstrates superior generalization across questions measuring the same construct.

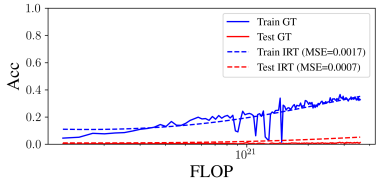


Figure 4: Pythia-12B checkpoints on WikiFact. Acc versus FLOP on the easy (train, blue) and difficult (test, red) question splits. Solid: GT scaling curves; dotted: IRT curves. The θ estimated from the easy question set generalizes to the hard question set, accurately predicting the scaling behavior on the hard question set, while the traditional approach fits dataset-specific scaling parameters.

This is a core property of IRT known in psychology as test-set invariance, meaning that ability estimates remain robust across subsets of varying difficulty. This feature is particularly important in the pre-training setting. For example, in an industrial setting where training and evaluation are handled by separate teams, increasing model ability with more compute causes CAT to adaptively choose more difficult questions for evaluation (Hofmann et al., 2025). By doing so, CAT ensures that different subsets are presented to the model, which can reduce contamination and lead to more reliable evaluation.

4.2 TEST-TIME ITEM RESPONSE SCALING LAW

Experimental Setup We collect two probability matrices, denoted as P_1^{testtime} and P_2^{testtime} . The matrix P_1^{testtime} contains the responses of 8 LLMs on 552 questions drawn from 6 multiple-choice benchmarks. For each entry, the empirical pass@1 is estimated by averaging over 10,000 samples, with queries performed under a few-shot setting and temperature 1. The matrix P_2^{testtime} contains the responses of 12 latest LLMs on 120 questions from 4 latest benchmarks, including both exact

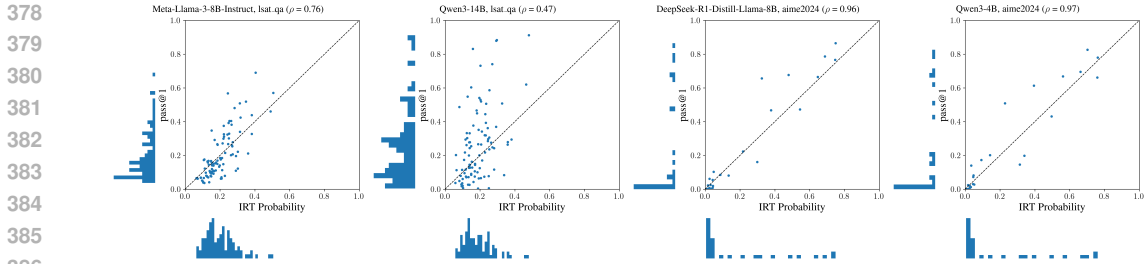


Figure 5: Consistency between (1) IRT-predicted probability with θ estimated from 50 or 30 questions and 50 samples (x -axis), and (2) $\text{pass}@1$ estimated from 10,000 or 2,500 samples (y -axis). Each point represents a question in the benchmark. From left to right, the four subplots are training LLM in P_1^{testtime} , test LLM in P_1^{testtime} , training LLM in P_2^{testtime} , and test LLM in P_2^{testtime} . IRT-predicted probabilities correlate closely with $\text{pass}@1$.

match and multiple-choice tasks. Here, the empirical $\text{pass}@1$ is estimated by averaging over 2,500 samples, with queries performed without few-shot examples but using chain-of-thought prompting at temperature 0.6.

Beta-IRT Calibration We adopt the Rasch model for both matrices, leaving out 4 LLMs for CAT. Question difficulty parameters z are calibrated on the remaining LLMs using the Beta loss. We report two correlation metrics for calibration performance: the Spearman correlation between the estimated difficulty z and the average empirical $\text{pass}@1$ of each question across the LLMs used for calibration, denoted as ρ_{train} ; and the Spearman correlation between z and the average empirical $\text{pass}@1$ across the LLMs left out for CAT, denoted as ρ_{test} . For P_1^{testtime} , we obtain $\rho_{\text{train}} = 0.97$ and $\rho_{\text{test}} = 0.80$. For P_2^{testtime} , we obtain $\rho_{\text{train}} = 0.99$ and $\rho_{\text{test}} = 0.95$.

Although leaderboard-calibrated difficulties are publicly available (Hofmann et al., 2025; Truong et al., 2025), we recalibrate question difficulties on the test-time probability matrices, because test-time scaling is typically conducted with a positive temperature to enable diverse sampling, whereas leaderboard evaluations are usually performed at temperature 0 for reproducibility. Our analysis shows that difficulties obtained under different evaluation setups can sometimes exhibit low correlation. For P_1^{testtime} , the questions overlap with those used in Truong et al. (2025). In Truong et al. (2025), question difficulties are calibrated from a binary response matrix of 42–91 test takers collected from the HELM leaderboard (Liang, 2023). We compare the estimated difficulties between our setting and theirs: across the six benchmarks, three exhibit high correlation while the other three do not, likely due to differences in evaluation setup (Figure 8). These results suggest there is hope to transfer difficulty estimates calibrated from leaderboards to test-time scaling scenarios, but they are not always reliable.

Beta-IRT CAT With calibrated question difficulties, we perform CAT using the Beta loss on both the LLMs included in calibration and those held out, with a sample budget of 50. For P_1^{testtime} , we set the question budget to 50, and for P_2^{testtime} , we set it to 30. Given the estimated LLM ability θ , we compute the correlation between the IRT-predicted probability $\sigma(\theta - z)$ and the empirical $\text{pass}@1$ estimated from all available samples. Figure 5 presents four subplots, corresponding to one training (included in calibration) and one test (held out) LLM on each of P_1^{testtime} and P_2^{testtime} . We report the Spearman correlation averaged across LLMs and datasets between IRT-predicted probability and $\text{pass}@1$: $\rho_{\text{train}}^{P_1} = 0.70$, $\rho_{\text{test}}^{P_1} = 0.53$, $\rho_{\text{train}}^{P_2} = 0.92$, $\rho_{\text{test}}^{P_2} = 0.88$. We observe that the IRT-predicted probabilities correlate closely with $\text{pass}@1$. However, when $\text{pass}@1$ is exactly zero, the IRT model fails to produce an exact zero probability, which introduces discrepancies in the law fitting process, as we describe next.

Scaling Law Fit We report 3 law curves on $\text{pass}@k$ or $-\log \text{pass}@k$ versus number of samples k in Figure 9: (1) the full unbiased (GT) curve serves as the ground truth. In this case, $\text{pass}@k$ is estimated from all available samples (10,000 or 2,500 samples) and all available questions using the unbiased and numerically stable estimator of Chen et al. (2021): $\widehat{\text{pass}}@k(i, j) = 1 - \binom{H - c_{ij}}{k} / \binom{H}{k}$, where H is the total number of available samples, c_{ij} is the number of correct samples of LLM i on question q_j among those samples. (2) In the sub $\text{pass}@1$ curve, $\text{pass}@k$ is estimated from subset questions (50 or 30 questions) and subset samples (50 samples): $\widehat{\text{pass}}@k(i, j) = \mathbb{E}_j[1 - (1 -$

432 $\hat{p}_{ij}^k]$, where $\hat{p}_{ij} = c_j/H$. (3) In the sub beta-IRT curve, \hat{z} is estimated from calibration, and $\hat{\theta}$ is
 433 estimated from subset questions (50 or 30 questions) and subset samples (50 samples). $\text{pass}@k$ is
 434 then estimated as $\text{pass}@k(i, j) = \mathbb{E}_j[1 - (1 - \hat{p}_{ij})^k]$, where $\hat{p}_{ij} = \sigma(\hat{\theta} - \hat{z})$. In the left half of
 435 Figure 9, we observe that the IRT law curves tend to achieve $\text{pass}@k = 1$ while the ground truth
 436 curves do not. This arises because IRT probabilities never reach exact zero: both θ and z are typically
 437 modeled as approximately normal, and even a large negative difference such as $\theta - z = -6$ yields
 438 $\sigma(-6) \approx 0.0025$. This behavior can be interpreted as an inherent limitation of IRT; one possible
 439 extension would be to introduce a prior that induces a binning effect. We also note that the ground-
 440 truth curves may be resolution-limited due to finite samples: if an LLM never answers a question
 441 correctly in the limited samples, the ground truth estimates become exactly zero.

442
 443 In psychometrics, questions that are never correctly answered are typically discarded because they
 444 provide no discriminatory power (Lord, 1980). Following this principle, we filter out questions with
 445 $\text{pass}@1 \leq 0.01$ and show empirically that this improves predictive reliability of IRT. After filtering,
 446 we obtain the right half of Figure 9, where the sub beta-IRT curve provides a closer estimate than
 447 the sub $\text{pass}@1$ curve under a limited query budget. We report the mean absolute errors (MAEs) of
 448 $-\log \text{pass}@k$ between the subset estimates and the ground-truth estimates for both IRT and $\text{pass}@1$.
 449 To highlight the relative advantage, we compute $\text{MAE}_{\text{pass}@1} - \text{MAE}_{\text{beta-IRT}}$ and visualize the results
 450 in Figure 10, where positive values (red) indicate superiority of IRT. Across nearly all LLMs and
 451 datasets, IRT achieves more reliable estimates of test-time scaling laws in an efficient manner, while
 452 being interpretable and generalizable.

453 **IRT Ability Estimates Generalize across**
 454 **Questions Measuring the same Construct**

455 We use the scaling performance of Qwen3-4B on Global MMLU Lite as a demonstration. We
 456 split the questions into an easy subset for training and a difficult subset for testing according
 457 to the calibrated difficulties. For the IRT, we first estimate the model’s ability parameter θ
 458 on the training set using pre-calibrated difficulties; we then combine θ with the pre-calibrated
 459 difficulties of the test set to predict the probability of correct responses. As shown in Figure
 460 6 (left), the IRT curves closely match the ground truth curves on both the training and test
 461 sets. This shows that θ generalizes across questions with different difficulties but measuring
 462 the same construct, while the traditional scaling law remains test set-specific. In Figure 6
 463 (right), we visualize $\text{pass}@1$ as a function of question difficulty z . The LLM ability θ
 464 estimated from the easy set generalizes effectively to the hard set, accurately pre-
 465 dicting $\text{pass}@1$ and giving accurate estimation for $\text{pass}@k$ scaling on more difficult questions,
 466 while the traditional approach remains dataset-specific.
 467
 468
 469
 470
 471
 472
 473
 474 producing a scaling curve that accurately predicts $\text{pass}@1$ on more difficult questions.

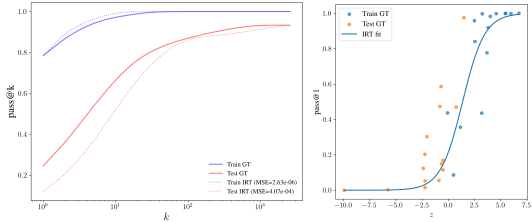


Figure 6: Qwen3-4B on Global MMLU Lite. **Left:** $\text{pass}@k$ versus k on the easy (train, blue) and difficult (test, red) question splits. Solid: GT scaling curves; dotted: IRT curves. **Right:** $\text{pass}@1$ as a function of question difficulty z . The LLM ability θ estimated from the easy set generalizes effectively to the hard set, accurately predicting $\text{pass}@1$ and giving accurate estimation for $\text{pass}@k$ scaling on more difficult questions, while the traditional approach remains dataset-specific.

475
 476 **5 DISCUSSION, LIMITATIONS, AND FUTURE WORK**

477 In the scaling laws literature, pre-training downstream curves are typically fit only to final check-
 478 points; by contrast, we fit to intermediate checkpoints of pretrained models. Our estimation of FLOP
 479 may be inaccurate because learning signals are nonuniform over training (e.g. due to warmup and
 480 decay schedules). Future work includes introducing a prior into IRT that induces a binning effect in
 481 test-time settings, fitting a shared latent ability that generalizes across benchmarks under the hypoth-
 482 esis that most benchmarks measure the ability to autoregress text (Truong et al., 2025; Kipnis et al.,
 483 2025), exploring alternative probabilistic models beyond IRT, extending to other scaling laws (e.g.,
 484 observational scaling law (Ruan et al., 2024), pre-training validation-loss scaling law (Kaplan et al.,
 485 2020), in-context scaling laws (Arora et al., 2025)), and extending IRT to non-binary assessments
 (Ostini & Nering, 2006).

REFERENCES

- 486
487
488 Aryaman Arora, Dan Jurafsky, Christopher Potts, and Noah D. Goodman. Bayesian scaling laws for
489 in-context learning, 2025. URL <https://arxiv.org/abs/2410.16531>.
- 490
491 Yasaman Bahri, Ethan Dyer, Jared Kaplan, Jaehoon Lee, and Utkarsh Sharma. Explaining neural
492 scaling laws. *arXiv preprint arXiv:2102.06701*, 2021.
- 493
494 Frank B Baker. *The basics of item response theory*. ERIC, 2001.
- 495
496 Edward Beeching, Clémentine Fourrier, Nathan Habib, Sheon Han, Nathan Lambert, Nazneen
497 Rajani, Omar Sanseviero, Lewis Tunstall, and Thomas Wolf. Open LLM leaderboard.
https://huggingface.co/spaces/open-llm-leaderboard-old/open_llm_leaderboard, 2023.
- 498
499 Akshita Bhagia, Jiacheng Liu, Alexander Wettig, David Heineman, Oyvind Tafjord, Ananya Harsh
500 Jha, Luca Soldaini, Noah A Smith, Dirk Groeneveld, Pang Wei Koh, et al. Establishing task
501 scaling laws via compute-efficient model ladders. *arXiv preprint arXiv:2412.04403*, 2024.
- 502
503 Stella Biderman, Hailey Schoelkopf, Quentin Gregory Anthony, Herbie Bradley, Kyle O’Brien, Eric
504 Hallahan, Mohammad Aflah Khan, Shivanshu Purohit, USVSN Sai Prashanth, Edward Raff, et al.
505 Pythia: A suite for analyzing large language models across training and scaling. In *International
506 Conference on Machine Learning*, pp. 2397–2430. PMLR, 2023.
- 507
508 Allan Birnbaum. Some latent trait models and their use in inferring an examinee’s ability. In
509 Frederic M. Lord and Melvin Novick (eds.), *Statistical Theories of Mental Test Scores*, pp. 392–
479. Addison-Wesley, Reading, MA, 1968.
- 510
511 R Darrell Bock and Murray Aitkin. Marginal maximum likelihood estimation of item parameters:
512 Application of an em algorithm. *Psychometrika*, 46(4):443–459, 1981.
- 513
514 Bradley Brown, Jordan Juravsky, Ryan Ehrlich, Ronald Clark, Quoc V Le, Christopher Ré, and
515 Azalia Mirhoseini. Large language monkeys: Scaling inference compute with repeated sampling.
arXiv preprint arXiv:2407.21787, 2024.
- 516
517 R. Philip Chalmers. mirt: A multidimensional item response theory package for the r environment.
518 *Journal of Statistical Software*, 48(6):1–29, 2012. doi: 10.18637/jss.v048.i06. URL <https://www.jstatsoft.org/index.php/jss/article/view/v048i06>.
- 519
520 Hua-Hua Chang. Psychometrics behind computerized adaptive testing. *Psychometrika*, 80(1):1–20,
521 2015.
- 522
523 Mark Chen, Jerry Tworek, Heewoo Jun, Qiming Yuan, Henrique Ponde de Oliveira Pinto, Jared
524 Kaplan, Harri Edwards, Yuri Burda, Nicholas Joseph, Greg Brockman, Alex Ray, Raul Puri,
525 Gretchen Krueger, Michael Petrov, Heidy Khlaaf, Girish Sastry, Pamela Mishkin, Brooke Chan,
526 Scott Gray, Nick Ryder, Mikhail Pavlov, Alethea Power, Lukasz Kaiser, Mohammad Bavarian,
527 Clemens Winter, Philippe Tillet, Felipe Petroski Such, Dave Cummings, Matthias Plappert, Fo-
528 tios Chantzis, Elizabeth Barnes, Ariel Herbert-Voss, William Hebgen Guss, Alex Nichol, Alex
529 Paino, Nikolas Tezak, Jie Tang, Igor Babuschkin, Suchir Balaji, Shantanu Jain, William Saunders,
530 Christopher Hesse, Andrew N. Carr, Jan Leike, Josh Achiam, Vedant Misra, Evan Morikawa, Alec
531 Radford, Matthew Knight, Miles Brundage, Mira Murati, Katie Mayer, Peter Welinder, Bob Mc-
532 Grew, Dario Amodei, Sam McCandlish, Ilya Sutskever, and Wojciech Zaremba. Evaluating large
language models trained on code, 2021. URL <https://arxiv.org/abs/2107.03374>.
- 533
534 Yangyi Chen, Binxuan Huang, Yifan Gao, Zhengyang Wang, Jingfeng Yang, and Heng Ji. Scaling
535 laws for predicting downstream performance in llms. *arXiv preprint arXiv:2410.08527*, 2024.
- 536
537 Florian E. Dorner, Yatong Chen, André F. Cruz, and Fanny Yang. Roc-n-reroll: How verifier imper-
538 fection affects test-time scaling, 2025. URL <https://arxiv.org/abs/2507.12399>.
- 539
Grattafiori et al. The llama 3 herd of models, 2024. URL <https://arxiv.org/abs/2407.21783>.

- 540 Samir Yitzhak Gadre, Georgios Smyrnis, Vaishaal Shankar, Suchin Gururangan, Mitchell Worts-
541 man, Rulin Shao, Jean Mercat, Alex Fang, Jeffrey Li, Sedrick Keh, Rui Xin, Marianna Nezhurina,
542 Igor Vasiljevic, Jenia Jitsev, Luca Soldaini, Alexandros G. Dimakis, Gabriel Ilharco, Pang Wei
543 Koh, Shuran Song, Thomas Kollar, Yair Carmon, Achal Dave, Reinhard Heckel, Niklas Muen-
544 nighoff, and Ludwig Schmidt. Language models scale reliably with over-training and on down-
545 stream tasks, 2024. URL <https://arxiv.org/abs/2403.08540>.
- 546 Leo Gao, Jonathan Tow, Baber Abbasi, Stella Biderman, Sid Black, Anthony DiPofi, Charles Fos-
547 ter, Laurence Golding, Jeffrey Hsu, Alain Le Noac’h, Haonan Li, Kyle McDonell, Niklas Muen-
548 nighoff, Chris Ociepa, Jason Phang, Laria Reynolds, Hailey Schoelkopf, Aviya Skowron, Lin-
549 tang Sutawika, Eric Tang, Anish Thite, Ben Wang, Kevin Wang, and Andy Zou. A framework
550 for few-shot language model evaluation, 12 2023. URL [https://zenodo.org/records/
551 10256836](https://zenodo.org/records/10256836).
- 552 David Heineman, Valentin Hofmann, Ian Magnusson, Yuling Gu, Noah A. Smith, Hannaneh Ha-
553 jishirzi, Kyle Lo, and Jesse Dodge. Signal and noise: A framework for reducing uncertainty in
554 language model evaluation, 2025. URL <https://arxiv.org/abs/2508.13144>.
- 555 Danny Hernandez, Jared Kaplan, Tom Henighan, and Sam McCandlish. Scaling laws for transfer.
556 *arXiv preprint arXiv:2102.01293*, 2021.
- 557 Joel Hestness, Sharan Narang, Newsha Ardalani, Gregory Diamos, Heewoo Jun, Hassan Kianinejad,
558 Md Mostofa Ali Patwary, Yang Yang, and Yanqi Zhou. Deep learning scaling is predictable,
559 empirically. *arXiv preprint arXiv:1712.00409*, 2017.
- 560 Jordan Hoffmann, Sebastian Borgeaud, Arthur Mensch, Elena Buchatskaya, Trevor Cai, Eliza
561 Rutherford, Diego de Las Casas, Lisa Anne Hendricks, Johannes Welbl, Aidan Clark, et al. Train-
562 ing compute-optimal large language models. *arXiv preprint arXiv:2203.15556*, 2022.
- 563 Valentin Hofmann, David Heineman, Ian Magnusson, Kyle Lo, Jesse Dodge, Maarten Sap, Pang Wei
564 Koh, Chun Wang, Hannaneh Hajishirzi, and Noah A. Smith. Fluid language model benchmarking,
565 2025. URL <https://arxiv.org/abs/2509.11106>.
- 566 John Hughes, Sara Price, Aengus Lynch, Rylan Schaeffer, Fazl Barez, Sanmi Koyejo, Henry Sleight,
567 Erik Jones, Ethan Perez, and Mrinank Sharma. Best-of-n jailbreaking, 2024. URL <https://arxiv.org/abs/2412.03556>.
- 568 Zhewei Kang, Xuandong Zhao, and Dawn Song. Scalable best-of-n selection for large language
569 models via self-certainty. *arXiv preprint arXiv:2502.18581*, 2025.
- 570 Jared Kaplan, Sam McCandlish, Tom Henighan, Tom B Brown, Benjamin Chess, Rewon Child,
571 Scott Gray, Alec Radford, Jeffrey Wu, and Dario Amodei. Scaling laws for neural language
572 models. *arXiv preprint arXiv:2001.08361*, 2020.
- 573 Alex Kipnis, Konstantinos Voudouris, Luca M. Schulze Buschoff, and Eric Schulz. metabench – a
574 sparse benchmark of reasoning and knowledge in large language models, 2025. URL <https://arxiv.org/abs/2407.12844>.
- 575 Percy et al. Liang. Holistic evaluation of language models. *Transactions on Machine Learning
576 Research*, 2023. URL <https://openreview.net/forum?id=iO4LZibEqw>.
- 577 Frederic M. Lord. *A Theory of Test Scores*. Psychometric Corporation, Richmond, VA, 1952.
- 578 Frederic M. Lord. *Applications of Item Response Theory to Practical Testing Problems*. Routledge,
579 1st edition, 1980. doi: 10.4324/9780203056615.
- 580 Nicholas Lourie, Michael Y Hu, and Kyunghyun Cho. Scaling laws are unreliable for downstream
581 tasks: A reality check. *arXiv preprint arXiv:2507.00885*, 2025.
- 582 Lovish Madaan, Aaditya K. Singh, Rylan Schaeffer, Andrew Poulton, Sanmi Koyejo, Pontus Stene-
583 torp, Sharan Narang, and Dieuwke Hupkes. Quantifying variance in evaluation benchmarks,
584 2024. URL <https://arxiv.org/abs/2406.10229>.

- 594 David Magis, Duanli Yan, and Alina A. von Davier. *Computerized Adaptive and Multistage Testing*
595 *with R*. Springer, Cham, 2017.
596
- 597 Ian Magnusson, Nguyen Tai, Ben Bogin, David Heineman, Jena D. Hwang, Luca Soldaini, Akshita
598 Bhagia, Jiacheng Liu, Dirk Groeneveld, Oyvind Tafjord, Noah A. Smith, Pang Wei Koh, and
599 Jesse Dodge. Datadecide: How to predict best pretraining data with small experiments, 2025.
600 URL <https://arxiv.org/abs/2504.11393>.
- 601 Rob R. Meijer and Michael L. Nering. Computerized adaptive testing: Overview and introduction.
602 *Applied Psychological Measurement*, 23(3):187–194, 1999.
603
- 604 Shubhra Mishra, Gabriel Poesia, Belinda Mo, and Noah D Goodman. Mathcamps: Fine-grained
605 synthesis of mathematical problems from human curricula. *arXiv preprint arXiv:2407.00900*,
606 2024.
- 607 Niklas Muennighoff, Alexander Rush, Boaz Barak, Teven Le Scao, Nouamane Tazi, Aleksandra
608 Piktus, Sampo Pyysalo, Thomas Wolf, and Colin A Raffel. Scaling data-constrained language
609 models. *Advances in Neural Information Processing Systems*, 36, 2024.
- 610 R. Ostini and M.L. Nering. *Polytomous Item Response Theory Models*. Polytomous Item Response
611 Theory Models. SAGE Publications, 2006. ISBN 9780761930686. URL <https://books.google.com.hk/books?id=wS8VEMtJ3UYC>.
- 612
613
- 614 Felipe Maia Polo, Lucas Weber, Leshem Choshen, Yuekai Sun, Gongjun Xu, and Mikhail
615 Yurochkin. tinybenchmarks: evaluating llms with fewer examples, 2024. URL <https://arxiv.org/abs/2402.14992>.
- 616
- 617 Felipe Maia Polo, Seamus Somerstep, Leshem Choshen, Yuekai Sun, and Mikhail Yurochkin. Sloth:
618 scaling laws for llm skills to predict multi-benchmark performance across families, 2025. URL
619 <https://arxiv.org/abs/2412.06540>.
620
- 621 Georg Rasch. *Probabilistic models for some intelligence and attainment tests*. ERIC, 1993.
- 622
- 623 Yangjun Ruan, Chris J Maddison, and Tatsunori Hashimoto. Observational scaling laws and the
624 predictability of language model performance. *arXiv preprint arXiv:2405.10938*, 2024.
- 625
- 626 Rylan Schaeffer, Hailey Schoelkopf, Brando Miranda, Gabriel Mukobi, Varun Madan, Adam
627 Ibrahim, Herbie Bradley, Stella Biderman, and Sanmi Koyejo. Why has predicting downstream
628 capabilities of frontier ai models with scale remained elusive? *arXiv preprint arXiv:2406.04391*,
2024.
- 629
- 630 Rylan Schaeffer, Joshua Kazdan, John Hughes, Jordan Juravsky, Sara Price, Aengus Lynch, Erik
631 Jones, Robert Kirk, Azalia Mirhoseini, and Sanmi Koyejo. How do large language monkeys get
632 their power (laws)?, 2025. URL <https://arxiv.org/abs/2502.17578>.
- 633
- 634 Sang Truong, Yuheng Tu, Percy Liang, Bo Li, and Sanmi Koyejo. Reliable and efficient amortized
635 model-based evaluation. *arXiv preprint arXiv:2503.13335*, 2025.
- 636
- 637 Wim J Van der Linden, Cees AW Glas, et al. *Computerized adaptive testing: Theory and practice*,
638 volume 13. Springer, 2000.
- 639
- 640 Mike Wu, Richard L Davis, Benjamin W Domingue, Chris Piech, and Noah Goodman. Variational
641 item response theory: Fast, accurate, and expressive. *arXiv preprint arXiv:2002.00276*, 2020.
- 642
- 643 Qiyuan Zhang, Fuyuan Lyu, Zexu Sun, Lei Wang, Weixu Zhang, Wenyue Hua, Haolun Wu, Zhihan
644 Guo, Yufei Wang, Niklas Muennighoff, et al. A survey on test-time scaling in large language
645 models: What, how, where, and how well? *arXiv preprint arXiv:2503.24235*, 2025.
646
647

648
649
650
651
652
653
654
655
656
657
658
659
660
661
662
663
664
665
666
667
668
669
670
671
672
673
674
675
676
677
678
679
680
681
682
683
684
685
686
687
688
689
690
691
692
693
694
695
696
697
698
699
700
701

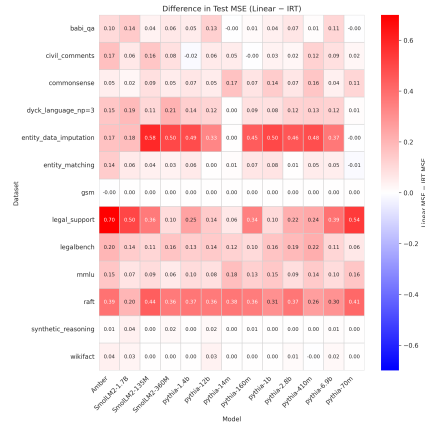


Figure 7: Heatmap of the difference in test MSE (Classic – IRT) across 13 benchmarks (rows) and 13 LLMs (columns) in Y_1^{pretrain} . Consistent positive (red) values indicate that the classical scaling law incurs higher error than the item response scaling law on the test set, demonstrating the latter’s superior generalization across question subsets with the same measurement objective but differing in difficulty.

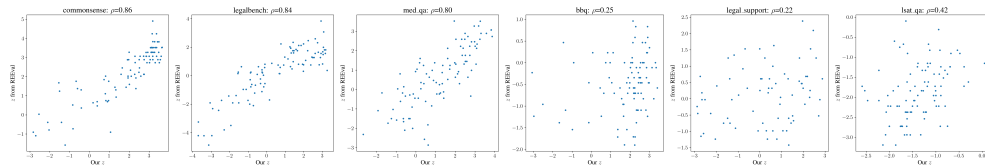


Figure 8: Consistency of question difficulty estimates between our calibration (x -axis) and Truong et al. (2025) (y -axis). Each point represents a question. Across the six benchmarks, three exhibit high correlation while the other three do not. There is hope to transfer difficulty estimates calibrated from leaderboards (temperature = 0) to test-time scaling scenarios (temperature > 0), but they are not always reliable.

A THE USE OF LARGE LANGUAGE MODELS (LLMs)

We used large language models (LLMs) as general-purpose assistive tools for two purposes: (1) polishing the writing of the paper, and (2) providing coding assistance. In all cases, the outputs generated by LLMs were carefully reviewed, verified, and modified by the authors before inclusion. The authors take full responsibility for all content presented in this paper.

B ADDITIONAL FIGURES

B.1 PRE-TRAINING DOWNSTREAM ITEM RESPONSE SCALING LAW

B.2 TEST-TIME ITEM RESPONSE SCALING LAW

